



ORIGINAL ARTICLE

In-situ electrochemical and piezogravimetric studies on the application of macrocyclic resorcinarene tetramer in the development of chemically-modified heavy metals ions detection platform in aqueous media



Larbi Eddaif^{a,b}, Ilona Felhósi^b, Abdul Shaban^{b,*}

^a Doctoral School on Materials Science and Technologies, Óbuda University, Faculty of Light. Industry and Environmental Engineering, Bp., Hungary

^b Functional Interfaces Research Group, Institute of Materials and Environmental Chemistry, Research Centre for Natural Sciences, Bp., Hungary

Received 7 December 2021; accepted 6 February 2022

Available online 9 February 2022

KEYWORDS

Calix[4]resorcinarene;
Mass-sensitive sensor;
Heavy metals;
Detection;
Voltammetric sensors

Abstract The new application of C-dec-9-enylcalix[4]resorcinarene (R_1), as an ionophore to detect heavy metals (HMs) cations (Cd^{2+} , Hg^{2+} , Cu^{2+} , and Pb^{2+}) in the aqueous media has been investigated through the preparation of an effective mass-sensitive sensor via the exploitation of a flow-type QCM-I technique. By adjusting the ions' amounts in model solutions over a wide range of concentrations, acquired changes in the oscillating frequency related to the loading of metal ions on the sensor's surface were gained, and thus favorable metrological parameters displaying the lowest detection limit (LOD) associated with copper ions (10 ppb). Simultaneously, a novel voltammetric sensor was prepared by modifying gold screen-printed electrodes (SPEs) with R_1 . Electrochemical characterization employing CV, SWV, and EIS was carried out, showing the success of the electrode modification. Then, the experimental conditions of supporting electrolyte, pH, accumulation time, and accumulation potential were optimized to achieve an enhanced detection. The R_1 @SPE sensor simultaneously detected the HMs (Cd^{2+} , Hg^{2+} , Cu^{2+} , Pb^{2+}), and the lowest LOD was associated with Pb^{2+} (0.19 ppb). The selectivity evaluation of the electrochemical sensor

* Corresponding author.

E-mail address: shaban.abdul@ttk.hu (A. Shaban).

Peer review under responsibility of King Saud University.



was performed by studying the effect of interferences majorly present in water sources (Mg^{2+} , Ni^{2+} , Zn^{2+} , Al^{3+} , and K^+) on the SWV detection signals, and it was revealed that the interfering ions did not affect the simultaneous detection of the studied HMs (RSD less than 5%), the voltammetric sensors also presented excellent repeatability and reproducibility (RSD less than 5%).

© 2022 The Author(s). Published by Elsevier B.V. on behalf of King Saud University. This is an open access article under the CC BY-NC-ND license (<http://creativecommons.org/licenses/by-nc-nd/4.0/>).

1. Introduction

Environmental contamination by heavy metals (HMs) is a hazard to the environment and is one of the most vital challenges in modern humanity (Li et al., 2013; Briffa et al., 2020). Trace levels of these toxicants if present in the ecosystem (soil, water surfaces... etc.) can cause dangerous effects on animal health (Woo et al., 2016). Mostly, entering the body via direct consumption of contaminated water and food beverages (Stewart et al., 2011), their toxicity is manifesting in the substitution of essential metals in the human body by interacting with enzymes and nucleic acids through binding to thiol groups of DNA, and so altering the body's functional properties (Lim and Schoenung, 2010; Stewart et al., 2011; Briffa et al., 2020).

The world health organization (WHO) and US Environmental Protection Agency (EPA) have taken giant steps to enlighten the awareness of the hazard and regulation of the thresholds concentration has been recommended (Mahajan B., 2021; USEPA, 2022). However, the identification and removal of these toxins from scarce water sources are vital necessities for communal protection.

There is a growing need for an ecologically safe, systematic, and novel methodology to remediate toxic heavy metals in water streams. The conventional approaches have limitations in terms of being noneconomic, requiring energy, and inefficiency. Common approaches to removing heavy metals from water sources are not widely offered over the world. Amongst the best effective progressive remediation processes, adsorption is extensively considered as the maximum effective method for handling a wide variety of heavy metals contaminants in aqueous systems. As a result, much research has focused on the use of low-cost adsorbents for heavy metal removal (Laghrib et al., 2021). For the remediation of environmental pollutants, sonophotocatalytic is a recently applied technique, where the complete improvement in the degradation activity can be credited to the synergic properties of sonolysis and photocatalysis, which lead to the formation of reactive free radicals (Theerthagiri et al., 2021; Yu et al., 2021).

The early environmental detection of HMs is crucial, their recognition in real samples is a difficult task owing to the complexity of various natural matrices (aquatic and river media), besides the very low concentrations of these ions, often below the detection limits of available techniques (Aragay et al., 2011; Elkhatat et al., 2021). On large scale, myriads of analytical procedures and physicochemical tools have been used to gather information on HM ions detection and monitoring in water sources, namely: FES, AAS, ICP-MS, ICP-OES, INAA, and UV/Vis (Kenawy et al., 2000; Hajiaghababaei et al., 2013; Jin and Ainliah, 2021), these approaches provide excellent and complete information in terms of metrological parameters related to sensitivity and selectivity. Nevertheless, the disadvantages and constraints are linked to the difficulty of use (need of skilled trained scientists) and time-consuming analysis (sampling, preparation, calibration, etc.).

At present, the reputation of sensors is well acknowledged, on account of their capability for conducting recognition investigations that were once dominated by analytical chemistry techniques, more advantages are offered by sensors as instrumentation low-cost, portability, data acquisition speed, technical reliability, real-time analyses, label-free onsite employment, and an overtime mapping-out of the target elements' existence in the studied environment, this later benefit is prohibitively costly when it comes to traditional detection procedures (Fadillah et al., 2020; Wu et al., 2019). The design, construction,

integration, and real application of HMs detection chemosensors, are comprehensively studied and reported in the literature, upon employing sensing platforms ranging from inorganic (Prochowicz et al., 2017) and nanomaterials (Deshmukh et al., 2018) to organic and macrocyclic elements (Bettazzi et al., 2012; Luo et al., 2019), by way of illustration calixarenes and resorcinarenes (Arora et al., 2007; Mei C. J. and Ahmad S. A. A., 2021), which had known ever-accelerating progress with regards to synthesis and structural alterations by modifying the cone dimensions. However, the mainstream of calixarene-based chemo-sensing platforms targeting HMs recognition in water matrices is of either electrochemical concept (voltammetry, amperometry, potentiometry, for instance, Ion-Selective-Electrodes (ISEs)) (Ahmadzadeh et al., 2015; Akl and Abd El-Aziz, 2016; Naik et al., 2021; Taghvaei-Ganjali et al., 2009; Pujol et al., 2014; Ebdelli et al., 2011; Göde et al., 2017; Nur Abdul Aziz et al., 2018) or Optical principle (fluorescence, colorimetry, etc.) (Chawla and Gupta, 2015; Echabaane et al., 2013; Erdemir et al., 2016; Lotfi et al., 2017; Mokhtari et al., 2011; Yang et al., 2019). In the field of environmental protection and monitoring, there is a tendency in sensing to use electrochemical impedance spectroscopy (EIS), cyclic voltammetry (CV), and SWV in combination with other measurement methods such as quartz crystal microbalance (QCM) (Briand et al., 2010).

The Quartz Crystal Microbalance with impedance measurements (QCM-I) involves two gold electrodes plated onto a piezoelectric thin quartz disk. Any adsorbed or desorbed mass on the gold surface causes a variation in the oscillation frequency (ΔF); an increase in mass causes a decrease in frequency and vice versa. This ΔF is proportional to the amount of variation in mass (Δm), as shown by the Sauerbrey equation (Eq. (1)) (Sauerbrey, 1959).

$$\Delta m = -C \cdot \frac{\Delta F}{n} \quad (1)$$

Where n is the overtone number and C is the mass sensitivity constant, which only depends on the physical properties of the quartz crystal.

QCM-I employs a network analyzer to permit continuous measurements of resonance parameters e.g. frequency, resonance curve, Full Width at Half Maximum variation ($\Delta FWHM$) calculations, along with monitoring the layer's viscoelastic properties via dampening energy evaluations, a.k.a. dissipation shifts (ΔD).

Mass-sensitive piezogravimetric techniques, as the QCM, showed their effectiveness in analytical applications for toxic metallic elements ions sensing by engaging numerous surface modifiers (Cao et al., 2011; Chen et al., 2011; Sartore et al., 2011; Emir Diltemiz, S. et al., 2017). However, apart from our published investigations (Eddaif et al., 2019a, 2020; Shaban and Eddaif, 2020), there's a lack of systematic studies dealing with the utilization of QCM to develop Calix-sensors for detecting HMs ions in aqueous solutions. Some consideration was given to the development of dicarboxyl-Calix[4]arene-based electrochemical sensing platform to detect lead ions in an aqueous solution (NurAbdul Aziz et al., 2018).

For that reason, this contribution aims to study the detection capability of a resorcinarene tetramer (C-dec-9-enylcalix[4]resorcinarene) towards toxic metallic ions, (Cd^{2+} , Hg^{2+} , Cu^{2+} , Pb^{2+}), in aqueous model solutions, by applying the QCM-I, and electrochemical methods (cyclic voltammetry (CV), and square wave voltammetry (SWV)).

2. Experimental

2.1. Chemicals

The used chemicals in the experimental part of this work are listed in Table 1. All chemicals from commercial sources were of analytical grade and used directly without further purification if no special instructions. All solutions were prepared and diluted by ultrapure water from the Milli-Q water purifier system.

2.2. Preparation of the ionophore

C-dec-9-enylcalix[4]resorcinarene (R₁) was prepared by dissolving resorcinol (0.23 mmol, 0.025 g) and 0.23 mmol of aldehyde (undec-10-enal) into absolute ethanol (240 mL) (Aoyama et al., 1989). The solution was cooled down to 0 °C, and 37 mL of concentrated HCl was added, after an hour of stirring, the solution was heated and refluxed for twelve hours. The recrystallization via methanol and a (1:1) mixture of acetone: hex-

ane, gave **R₁** as a yellowish-orange solid (Yield: 49 %, m. p.:277 °C).

The resorcinarene tetramer was synthesized based on the acid-catalyzed cyclo condensation reactions, viz.: C-dec-9-enyl calix[4]resorcinarene (**R₁**), and was the subject of full structural characterization studies employing FT-IR, ¹H/ ¹³C NMR, powder XRD, and thermal analyses (Eddaif et al., 2019b). The chemical structure of (**R₁**) is presented in Fig. 1.

2.3. Pretreatments of electrodes

For the piezogravimetric analysis, AT-cut gold-plated quartz crystal resonators (QCR) with a 5 MHz fundamental frequency and 14 mm diameter, were used. The QCR's gold surface was rinsed by acetone (a.r., Reanal), washed with piranha solution (H₂O₂ (30%) and H₂SO₄ (96%) in a ratio of (1:2) for 10 min, rigorously rinsed with Milli-Q water, and finally, let dry at room temperature inside a desiccator.

For electrochemical experiments, screen-printed gold electrodes (Pine Research, USA) were used. The electrodes (Pine

Table 1 List of used chemicals in the experimental work.

| Name | Formula | Characteristics | Purchased from |
|---------------------------------------|--|-------------------------------|--------------------------------|
| Hydrogen peroxide (30%) | H ₂ O ₂ | Extra pure | Molar Chemicals KFT |
| Tetrahydrofuran (THF) | C ₄ H ₈ O | Extra pure | Molar Chemicals KFT |
| Sulfuric acid (96%) | H ₂ SO ₄ | Analytical grade | Molar Chemicals KFT |
| Hydrochloric acid (37%) | HCl | Analytical grade | Molar Chemicals KFT |
| Glacial acetic acid (+99 %) | CH ₃ CO ₂ H | Analytical grade | Sigma-Aldrich |
| Sodium hydroxide (+98 %) | NaOH | Analytical grade | Sigma-Aldrich |
| Ammonium acetate | CH ₃ CO ₂ NH ₄ | Analytical grade | Merck |
| Ammonia (25%) | NH ₃ | Analytical grade | Molar Chemicals KFT |
| Nitric acid (65%) | HNO ₃ | Analytical grade | Molar Chemicals KFT |
| Hellmanex III | — | Alkaline cleaning concentrate | Hellma GmbH & Co. KG (Germany) |
| Pb(II) nitrate | Pb(NO ₃) ₂ | 99.99% | Sigma-Aldrich |
| Cd(II) nitrate tetrahydrate | Cd(NO ₃) ₂ ·4H ₂ O | 98% | Sigma-Aldrich |
| Hg(II) chloride | HgCl ₂ | 99.5% | Sigma-Aldrich |
| Cu (II) nitrate trihydrate | Cu(NO ₃) ₂ ·3H ₂ O | Extra pure | Sigma-Aldrich |
| Mg(II) chloride hexahydrate | MgCl ₂ ·6H ₂ O | Analytical grade | Molar Chemicals KFT |
| Al(III) nitrate nonahydrate | Al(NO ₃) ₃ ·9H ₂ O | Analytical grade | Sigma-Aldrich |
| Ni(II) nitrate hexahydrate | Ni(NO ₃) ₂ ·6H ₂ O | Analytical grade | Reanal |
| K(II) sulfate | K ₂ SO ₄ | 99.5 % | Molar Chemicals KFT |
| K(I) chloride | KCl | + 99 % | Sigma-Aldrich |
| Trans-2,cis-6-nonadienal (+96%) | C ₉ H ₁₄ O | d = 0.866 | Sigma-Aldrich |
| Undecylenic aldehyde (95%) | C ₁₁ H ₂₀ O | d = 0.81 | Sigma-Aldrich |
| (S)-(-)-α-Methylbenzylamine (p ≥ 98%) | C ₈ H ₁₁ N | d = 0.952 | Fluka Chemie GmbH |
| (R)-(+)-α-Methylbenzylamine (p ≥ 98%) | C ₈ H ₁₁ N | d = 0.952 | Fluka Chemie GmbH |
| Dodecanal | C ₁₂ H ₂₄ O | d = 0.831 | Sigma-Aldrich |
| Paraformaldehyde | HO(CH ₂ O) _n H | Reagent grade | Molar Chemicals KFT |

research, USA) were composed of three electrodes printed system (2 mm OD gold working electrode, a U-shaped large gold counter electrode, and an Ag/AgCl reference electrode) connected to the potentiostat through a connector cable. Potential contaminants on screen-printed electrodes (SPEs) were removed by cyclic voltammetric cleaning by applying 20 CV cycles at 100 mV.s^{-1} scan rate in $0.05 \text{ M H}_2\text{SO}_4$ solution in the potential range from -1.5 to $+0.5 \text{ V}$. The electrochemical cleaning resulted in stable voltammograms, and the cleaned SPEs were rinsed with Milli-Q water (resistivity/conductivity at $25 \text{ }^\circ\text{C}$: $18 \text{ M}\Omega.\text{cm}^{-1} / 5.5 \times 10^{-6} \text{ S.m}^{-1}$) and placed in a desiccator at room temperature until further use.

2.4. Ionophore immobilization on the gold sensing area

For immobilizing the macrocycle onto the gold sensing area, \mathbf{R}_1 was dissolved in chloroform (a.r., Molar Chemicals Kft) (2 mg.mL^{-1}). With subsequent intensive drop-casting of the ionophore solution on the clean QCR's gold surface ($10 \text{ }\mu\text{L}$) and screen-printed electrodes ($2 \text{ }\mu\text{L}$), the resorcinarene based sensing platforms were fabricated. The modified electrodes were later dried at room temperature and kept inside a desiccator ($25 \text{ }^\circ\text{C}$) awaiting further use.

2.5. QCM-I measurements

The HMs salts (Sigma- Aldrich) ($\text{Pb}(\text{NO}_3)_2$, $\text{Cd}(\text{NO}_3)_2$, HgCl_2 , and $\text{Cu}(\text{NO}_3)_2$) were mixed at convenient amounts, with Milli-Q water, to prepare the water model solutions with concentration range $5\text{--}1000 \text{ ppm}$. Label-free onsite real-time QCM-I detection experiments were performed utilizing the QCM-I instrument (MicroVaccum Ltd, Hungary). The device's resonance sensitivity in the liquid is 0.2 Hz , the dissipation sensitivity is 1.10^{-7} , and the mass sensitivity is $\leq 1 \text{ ng.cm}^{-2}$.

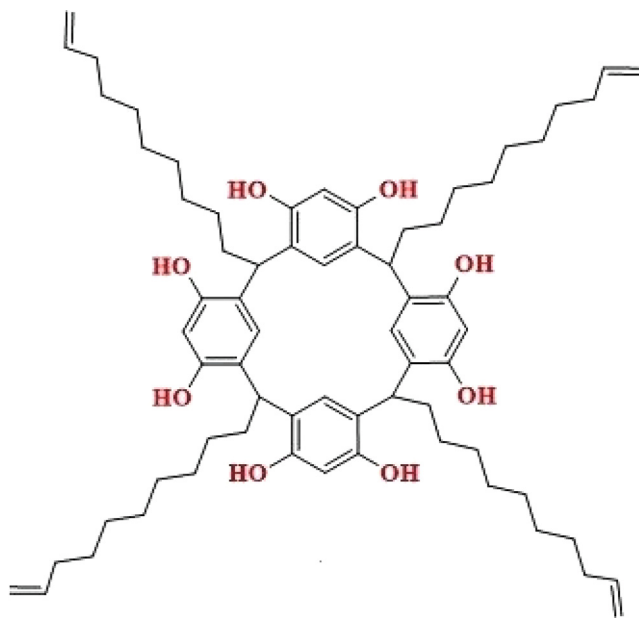


Fig. 1 Molecular structure of C-dec-9-enylcalix[4]resorcinarene (\mathbf{R}_1).

The apparatus enclosed a $40 \text{ }\mu\text{L}$ flow-cell and was automatically thermostated ($25 \text{ }^\circ\text{C}$), and the applied flowrate was $200 \text{ }\mu\text{L.min}^{-1}$ for injecting the HMs solutions by a peristaltic pump. Experiments were computer-controlled using the BioSense Software V. 3.1 (MicroVaccum Ltd). The data were recorded for selected overtones $n = 1, 3, 5,$ and 7 , on behalf of $5, 15, 25,$ and 35 MHz frequencies, respectively. The normalization of ΔF is accomplished by dividing the change in the measured values by the used overtone number (n) (Eq. (2)):

$$\Delta F_N = \frac{\Delta F n}{n} \quad (2)$$

2.6. Electrochemical experiments

The voltammetric tests, viz. cyclic voltammetry (CV) and square wave voltammetry (SWV) were performed using a Gamry interface 1010E potentiostat/galvanostat apparatus controlled by the Gamry inst. framework software, whereas the electrochemical impedance spectroscopy (EIS) experiments were carried out using a Solartron frequency analyzer/electrochemical interface system (1250/1286) controlled by the ZPlot software.

2.6.1. Electrochemical characterization

EIS is a well-known sensing method to examine the statuses of affinity reactions on electrode surfaces established on the interaction of the analyte with the electrical double-layer or the perturbation of the redox reactions. Electrochemical processes that take place around the vicinity of an electrode surface can be analyzed using the EIS technique. EIS in chemosensor applications focuses on surface actions taking place in a frequency region typically from mHz to kHz .

Prior to the electrochemical characterization tests, the SPE was immersed into the cell containing 0.2 M HCl and the target metal ions with a 3 min stirring time before their accumulation at open circuit potential (OCP). The electrochemical characterization of the bare/modified electrodes in the absence/presence of 1 ppm of HMs dissolved in 0.2 M HCl solution was completed employing the following conditions:

In the case of EIS, the *ac* voltage was set to $V_{ac} = 10 \text{ mV}$ amplitude sine wave signal, whereas the *dc* voltage (bias) remained at the open-circuit potential (OCP) in order to stay in the linear region of the Butler-Volmer equation. The applied frequency range was from 65 kHz to 1 Hz .

Cyclic voltammetry is a measurement procedure in which the potential is driven between the working electrode (WE) and the reference electrode in the form of slow cyclic changing triangle-shaped voltages. At the same time, the current between WE and counter electrode (CE) is recorded which produces an exact analysis of potential oxidizing (Ox) and reducing (Red) species present in the solution. Forward and back CV scans were performed in the potential range from -0.75 V to $+0.5 \text{ V}$ at a scan rate = 50 mV.s^{-1} . Square wave voltammetry measurements were executed at frequency = 15 Hz , deposition time = 60 s , deposition potential of -1V within the potential window from -1 to $+0.5 \text{ V}$.

2.6.2. Experimental parameters optimization

Aiming to enhance the detection capacity of the prepared sensor towards various heavy metals, the physicochemical param-

eters having a direct influence on the SWV signals were optimized. SWV is a fast electroanalytical method that depends on the frequency (Hz) and step height (mV). It generates a peak-shaped symmetrical voltammogram. The current is recorded twice during each cycle of the square wave, once at the end of the forward pulse and once at the end of the reverse pulse. The concentration of the investigated HM ions is proportionate to the current peak. It has a high sensitivity because the current peak is larger than the oxidation/reduction separated signals.

The influence of various supporting electrolytes was examined in order of choosing the most suitable one for offering the highest detection magnitude. The square wave voltammetry conditions were similar to those employed in the electrochemical characterization. The studied electrolytes are HCl 0.2 M ($\text{pH}_i = 0.7$), KCl 0.2 M ($\text{pH}_i = 6.8$), and acetate buffer ACB 0.2 M ($\text{pH}_i = 5.3$), prepared by mixing 15.4 g of ammonium acetate and 2.06 mL of glacial acetic acid in 990 mL of distilled water.

The electrolytic medium's pH is highly affecting the interactions between the sensing platform and the target ions. Therefore, the detection response in 0.2 M HCl has been investigated by changing the pH values from 0.7 to 8. The pH was adjusted by 0.1 M NaOH ($\text{pH}_i = 13$) and was monitored by the ADWA AD8000 digital pH meter. The SWV conditions were similar to those employed in the electrochemical characterization.

The optimization of the accumulation time and potential effects on the \mathbf{R}_1 @SPE sensing platforms were studied within

the time-frame of 30–180 s and within potential values from -2V to -1V , with the purpose to produce higher signals and improved detection performance.

2.6.3. Simultaneous electrochemical detection of heavy metals (Calibration studies)

The detection capability of the \mathbf{R}_1 @SPE sensor towards various heavy metals ions, with concentrations ranging from 1 to 100 ppb, was examined under the optimized circumstances, for the determination of the statistical detection characteristics (linear ranges, detection, and quantification limits).

2.6.4. Interference studies

The most common potential interfering metals cations were Al^{3+} , Fe^{3+} , Fe^{2+} , Mg^{2+} , Co^{2+} , Mn^{2+} , Zn^{2+} , Pb^{2+} , Cd^{2+} , Sn^{2+} , and Ni^{2+} , as studied by Pratiwi and coworkers (Pratiwi et al., 2017), where they showed that the presence of common metal ions did not interfere with Cu^{2+} detection within reasonable tolerance ratios.

The selectivity of the \mathbf{R}_1 @SPE platform for Pb^{2+} , Cd^{2+} , Cu^{2+} , Hg^{2+} ions was evaluated in the presence of other metals frequently present in environmental samples, Al^{3+} , K^+ , Mg^{2+} , Zn^{2+} , and Ni^{2+} , usually present in water sources. Interfering ions of 4 ppm (40 folds compared to target ions) were added to 0.2 M HCl containing 100 ppb of heavy metals ions (Pb^{2+} , Cd^{2+} , Cu^{2+} , Hg^{2+}), and SWV detection studies were performed under optimized conditions.

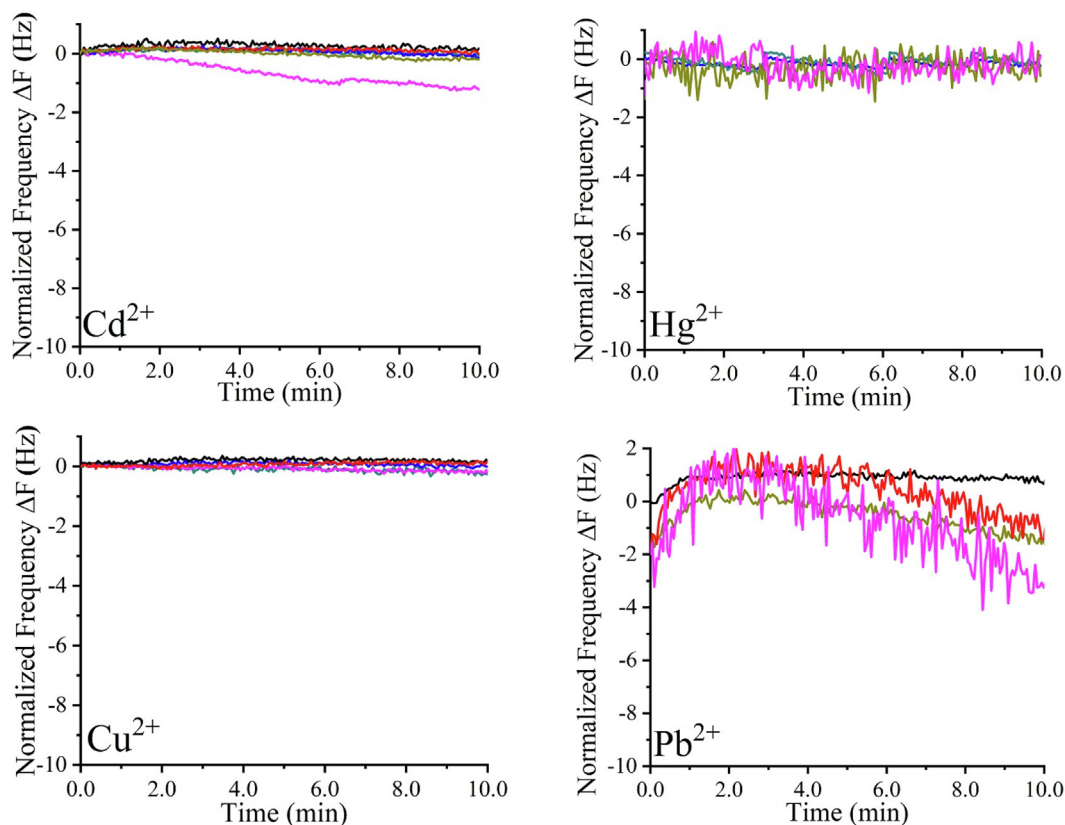


Fig. 2 Normalized frequency (a) and dissipation shifts (b) of unmodified QCR against various heavy metals concentrations (0, 5, 25, 250, 500, and 1000 ppm) in time.

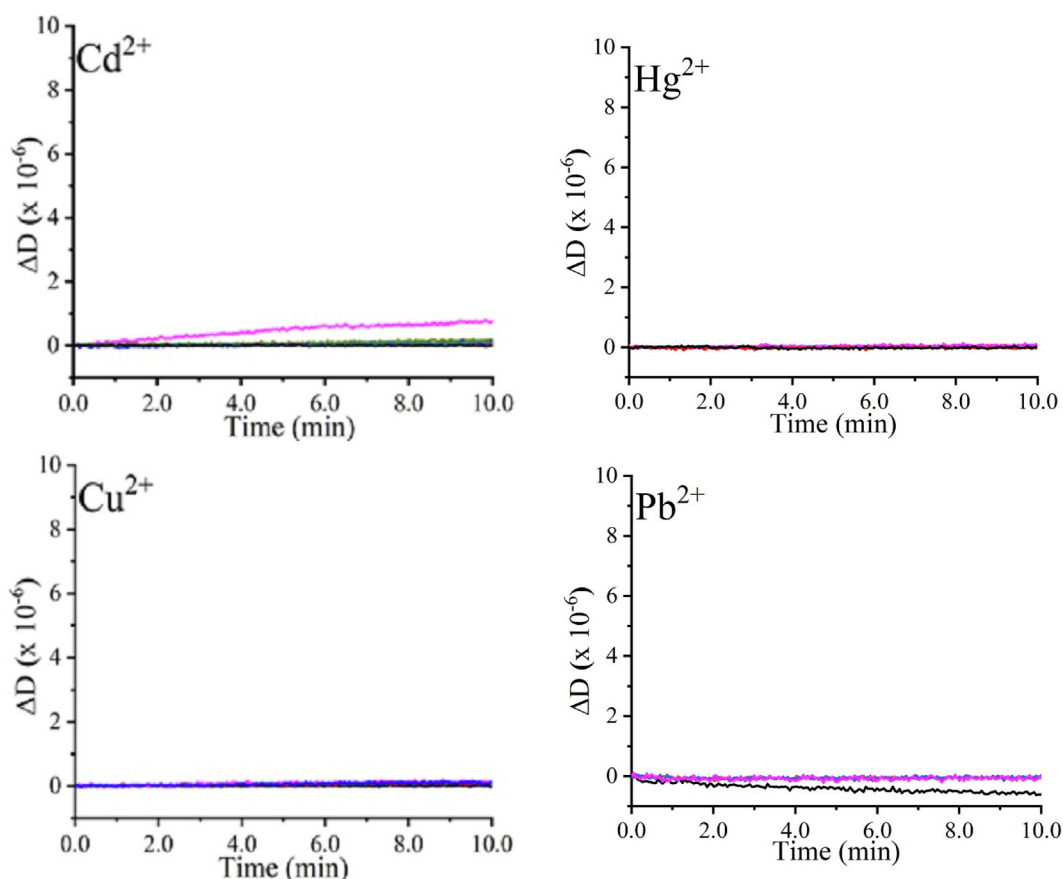


Fig. 2 (continued)

2.6.5. Reproducibility and repeatability

To evaluate the repeatability of the fabricated sensor, its sensing platform was employed for detecting 100 ppb of heavy metals under optimized conditions by running 3 successive measurements. Hence, for assessing the reproducibility, three different SPEs modified by \mathbf{R}_1 were used to detect 100 ppb of heavy metals ions under optimized conditions. The standard deviation (RSD) was calculated to evaluate these parameters.

3. Results and discussion

3.1. QCM-I studies

3.1.1. Effect of heavy metals ions on unmodified quartz crystal electrodes

As a first step, the effect of heavy metal ion concentration was studied on the bare gold electrodes of quartz crystals, frequency and dissipation shifts through the in-situ QCM-I measurements were recorded. As seen in Fig. 2, the unmodified gold electrodes did not detect any loading of the heavy metals ions on the gold surface ($\Delta F \approx 0$) (Fig. 2a). A rigid character of the electrodes' surfaces was dominant, as no changes in dissipation energy were obvious ($\Delta D \approx 0$) (Fig. 2b). Though, some fluctuations were existing in the majority of plots, which are explained by the electrode's surface wetting due to straight exposure to heavy metals solutions. The inability of bare gold

surfaces to sense heavy metals ions proves that neither physical nor chemical interactions have occurred. It is worth mentioning that the chemical interactions are crucial in increasing the quartz crystal's sensitivity, where taking advantage of detection networks is compulsory.

3.1.2. Effect of heavy metals ions on the prepared piezogravimetric sensor

Targeting water environmental detection via applied in-situ QCM-I analysis, drop-coated gold electrodes using \mathbf{R}_1 as sensing platforms were constructed, aiming at evaluating their HMs detection capabilities in model solutions modified via adding toxic metallic elements. Fig. 3 illustrates the normalized frequency (a) and dissipation variations (b) (ΔF_N and ΔD_N) of Calix-chemosensor \mathbf{R}_1 in time. Whereas, Table.2 contains a summary of the ΔF_N and ΔD_N values collected from endpoints of the detection plots.

From Fig. 3, it is apparent that the heavy metals ions sensing through the application of Calix-based piezogravimetric sensors disclosed its success since the decrease in frequency with increasing the ions amounts is directly related to the mass loading of heavy metals ions on the quartz crystal sensor's surface (Fig. 3a).

The resorcinarene thin films' viscoelastic properties were monitored simultaneously with frequency variations, by recording energy dissipation shifts based on oscillation amplitude variations in time (via ring-down method) (Fig. 3b).

Commonly, the higher is the dissipation shift ($\Delta D > 2.10^{-6}$), the softer is the adlayer, and thus the viscoelastic model description deviates from the Sauerbrey model conditions as previously indicated by (Eq. (1)).

3.1.3. Piezogravimetric sensor's metrological parameters and ionic selectivity

The sensors' pertinence rest on detection features manifesting in sensitivity (S), linear range (L.R.), detection, and quantification limits (LOD and LOQ). However, excellent sensing characteristics are considered as small LODs and LOQs, high sensitivities, and wide LRs. To evaluate the metrological parameters, the dynamic ranges based on ΔF_N variations for ionophore \mathbf{R}_1 based piezogravimetric sensor are presented in Fig. 4, whereas Table 3 is recapitulating LRs, LODs, LOQs, and sensitivities of the Calix-based chemosensor.

The LODs and LOQs were calculated from $\text{LOD} = 3.3\sigma/S$ and $\text{LOQ} = 10\sigma/S$, where σ is the standard deviation and S is the linear range's slope or the sensitivity. The developed detection platforms showed respectful sensing characteristics (wide LRs, noble sensitivities, low LODs, and LOQs), based on frequency variations. The obtained LODs in the case of Hg^{2+} , Pb^{2+} , and Cd^{2+} ions were slightly higher than the recommended thresholds. Nonetheless, in the case of Cu^{2+} , the chemosensor was sensitive since it produced an inferior LOD to limits stated by WHO (2 ppm) and USEPA (1.3 ppm). The selectivity evaluation based on frequency shifts (Fig. 4) indicates that \mathbf{R}_1 is selective to mercury and cadmium ions.

3.1.4. Hypothetical interpretation of the ionophore adsorption on QC gold surface

Ensuring the best performance of the developed piezogravimetric sensor, resorcinarene detection platforms should be well attached and well-constructed, the ligands affixation on the quartz crystal surface is then ascertained by electrostatic interactions (Mainly VDW -Van der Waals- dispersion forces with a quantum mechanical nature, manifesting in dipoles produced via quantum fluctuations) between heteroatoms, i.e. O, aromatic cycles' electrons, end carbon chain double bonds, and the gold surface. As appraised by the work of Reimers and coworkers (Reimers et al., 2017), aromatic cycles and carbon chains interact strongly with coinage metals-based surfaces such as gold, resulting in their adsorption via VDW interactions comparable to covalent attachment in terms of strength. For a clarified overview, the free gold atoms can either react with their 'd' or 's' orbitals ($d^{10}s^1$ as electronic valence configuration), due to their high reactivity and capability of covalent bonding to carbon atoms forming single, double, and even triple bonds (Tang and Jiang, 2015; Zaba et al., 2014). However, when gold atoms are attached forming a single Au-Au bond via s-s orbitals, their reactivity weakens, which is the case of noble gold surfaces, yet, this fact does not disturb the VDW dispersive forces for those bonds formed via 'd' orbitals of gold surface and carbon atoms as an example (Chaudhuri et al., 2009; Reimers et al., 2016). Besides the later interaction, electron flow between O, and gold surface atoms is ensured through a moment dipole polarization creating an electron density stream.

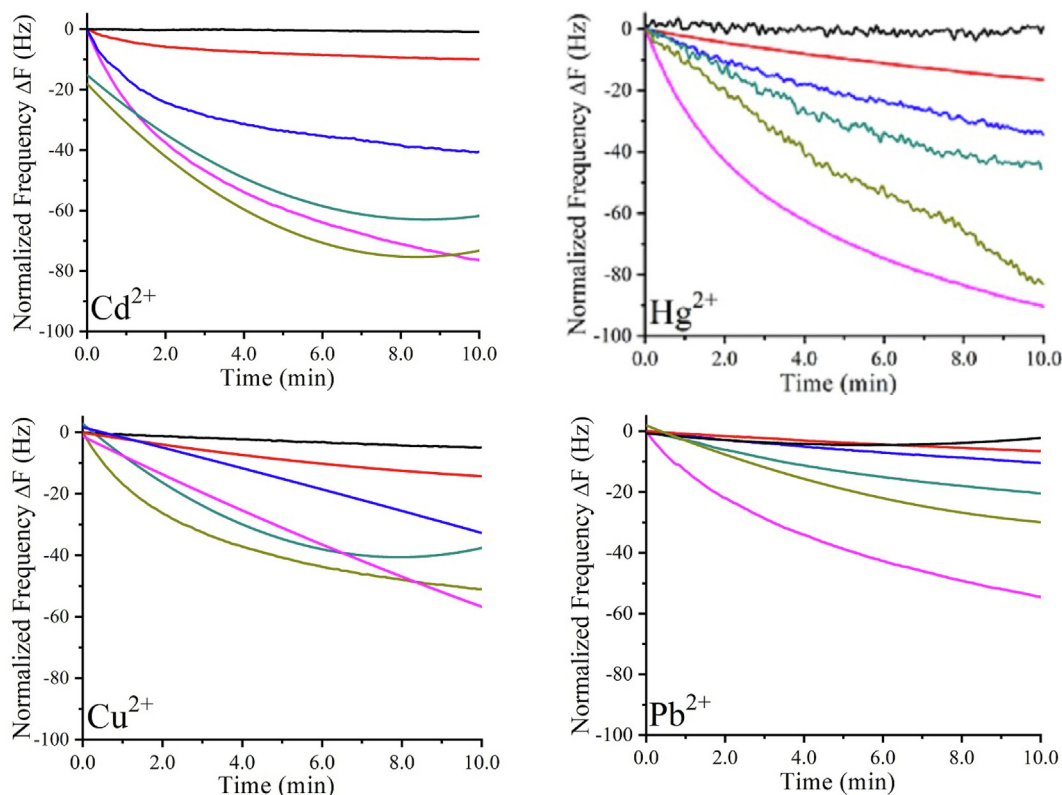


Fig. 3 Normalized frequency (a) and dissipation shifts (b) for ionophore \mathbf{R}_1 modified QCR against various heavy metals concentrations (0, 5, 25, 250, 500, and 1000 ppm) in time.

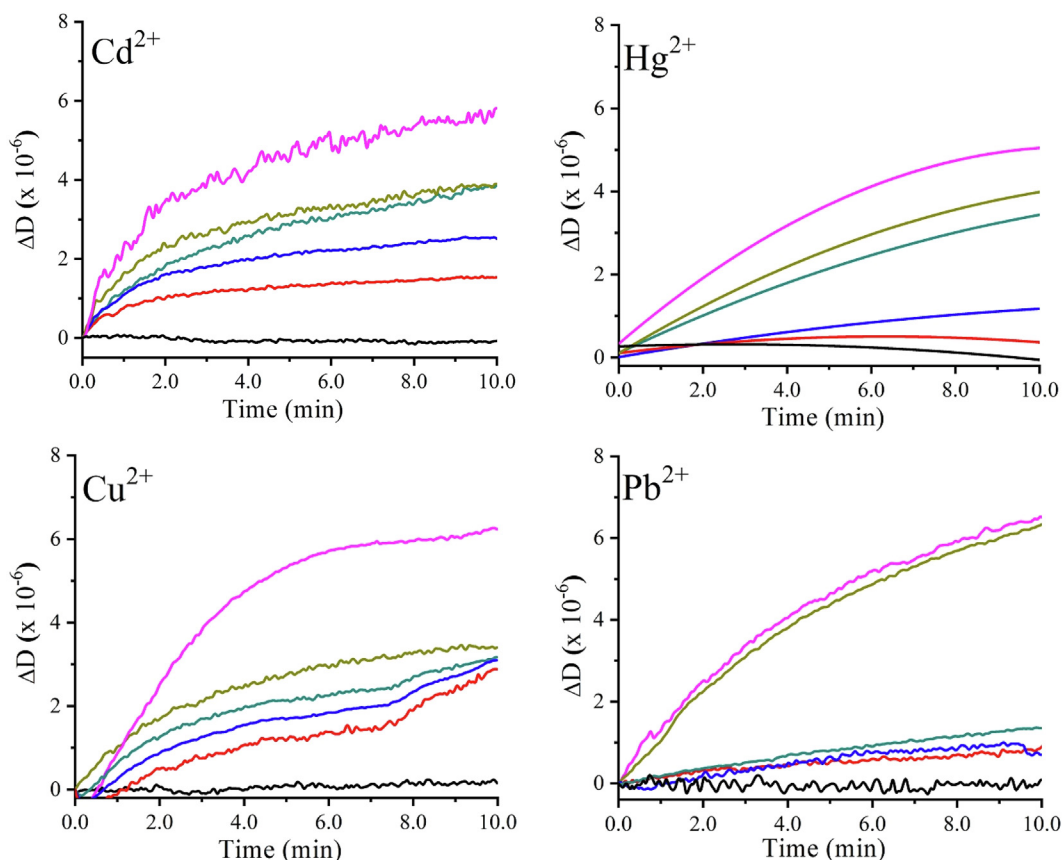
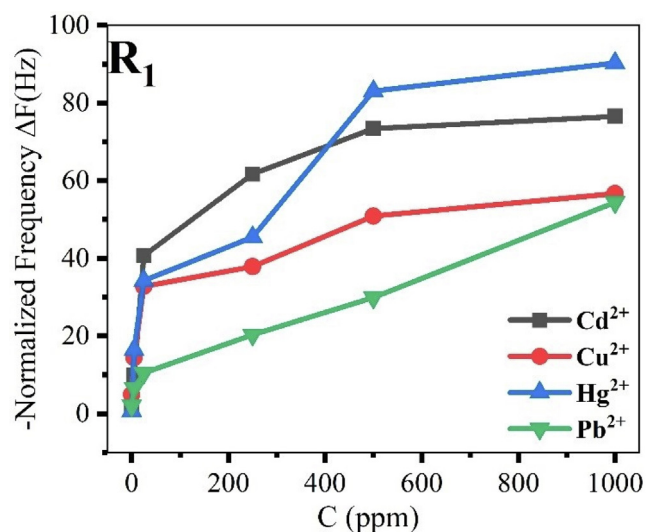


Fig. 3 (continued)

Table 2 Normalized frequency and dissipation data for ionophore (R_1) based QCM sensor against various HM amounts.

| Metal ions | C (ppm) | ΔF (Hz) | ΔD ($\times 10^{-6}$) |
|------------|---------|-------------------|---------------------------------|
| Cd^{2+} | 0 | -1.14 ± 0.01 | 0.07 ± 0.02 |
| | 5 | -9.85 ± 0.04 | 1.54 ± 0.01 |
| | 25 | -40.70 ± 0.30 | 2.51 ± 0.03 |
| | 250 | -61.70 ± 0.90 | 3.83 ± 0.04 |
| | 500 | -73.46 ± 0.78 | 3.84 ± 0.07 |
| | 1000 | -76.55 ± 0.50 | 5.79 ± 0.90 |
| Cu^{2+} | 0 | -4.94 ± 0.03 | 0.12 ± 0.01 |
| | 5 | -14.42 ± 0.02 | 2.87 ± 0.04 |
| | 25 | -32.76 ± 0.07 | 3.09 ± 0.02 |
| | 250 | -37.91 ± 0.01 | 3.19 ± 0.03 |
| | 500 | -50.91 ± 0.09 | 3.40 ± 0.09 |
| | 1000 | -56.68 ± 0.10 | 6.24 ± 0.10 |
| Hg^{2+} | 0 | -0.65 ± 0.08 | 0.05 ± 0.01 |
| | 5 | -16.46 ± 0.03 | 0.36 ± 0.01 |
| | 25 | -34.27 ± 0.06 | 1.17 ± 0.02 |
| | 250 | -45.47 ± 0.07 | 3.43 ± 0.03 |
| | 500 | -83.06 ± 0.13 | 3.98 ± 0.06 |
| | 1000 | -90.32 ± 0.01 | 5.05 ± 0.04 |
| Pb^{2+} | 0 | -2.13 ± 0.02 | 0.05 ± 0.03 |
| | 5 | -6.55 ± 0.01 | 0.87 ± 0.02 |
| | 25 | -10.48 ± 0.07 | 0.71 ± 0.01 |
| | 250 | -20.36 ± 0.09 | 1.35 ± 0.04 |
| | 500 | -29.90 ± 0.04 | 6.31 ± 0.22 |
| | 1000 | -54.44 ± 0.03 | 6.51 ± 0.34 |

**Fig. 4** Dynamic ranges for ionophore R_1 based on the normalized frequency variation.

3.2. Electrochemical studies

3.2.1. Electrochemical characterization

Cyclic voltammetry, besides providing exact analysis of possible oxidizing and reducing species existing in the solution, can offer an opportunity to characterize the electrical double-layer,

Table 3 Metrological parameters of Calix-QCM sensor based on ΔF_N .

| HMs | LR (ppm) | S (Hz/ppm) | LOD (ppm) | LOQ (ppm) |
|------------------|-------------|---------------|--------------|--------------|
| Cd ²⁺ | 2–25 | 1.571 | 0.61 | 1.83 |
| Cu ²⁺ | 0.5–25 | 1.056 | 0.01 | 0.03 |
| Hg ²⁺ | 3–25 | 1.215 | 0.88 | 2.64 |
| Pb ²⁺ | 2–1000 | 0.045 | 0.47 | 1.42 |

since the current is influenced by charging the capacitive load. The heights of the current peaks show evidence of chemical activity, while the area below the current–voltage curve gives info about the charge transfer capacity of the surface (Arfin, 2021).

The behavior of the R_1 based electrochemical sensor was preliminarily examined employing CV. Fig. 5A presents the CV signatures of the bare and modified electrodes in the presence and absence of ions.

Starting the forward scan at a potential (-0.750 V), the potential increases during the voltammetry curve. The anodic reduction affects the CV curve by increasing current density and showing peaks for Cd, Pb, Cu, and Hg ions at the respected potentials. Due to the diffusion of reduced species at the vicinity of the anode, current density decreases until the inverse potential (+0.500 V) is reached. The back scan starts by decreasing the potential between the electrodes which leads to oxidizing of the reduced species at the cathode having an impact on the current density with cathodic peaks at the respected potential values. Further decrease of the voltage indicates the diffusion limitation until the minus reverse potential is reached. The applied voltage is increased until the starting potential (-0.750 V) is reached again and the potential cycle is finished. Besides the current density value at the peak, the potentials for the anodic and cathodic peaks and their difference are also considered as important parameters of a CV illustration.

As displayed in Fig. 5A, no significant analytical signals (redox peaks) appeared in the absence of ions for the bare (a) and modified electrode (c) in 0.2 M HCl. However, bare gold electrode (b) presented moderate responses when the ions were added to the electrolytic medium, and further modifications of the electrode with ionophore R_1 (d) have enhanced the well-defined oxidation current peaks of heavy metals ions on their respective potentials. However, the cathodic reduction peaks of HMs are not well-separated and intense as the anodic ones. The observed increase in the CV current peaks of heavy metals after the electrode modification is owing to the fast electron-transfer rate at the R_1 @SPE platform and its conductive nature, besides the complexation process between the heavy metals ions in the electrolyte and the impregnated resorcinarenes on the electrodes.

Besides having high sensitivity, SWV can achieve very low detection limits by applying effective discrimination against the charging background current. The SWV signatures of the bare and modified electrodes in the presence and absence of heavy metals were also studied to complement the cyclic voltammetry characterization and are shown in Fig. 5B. The SWV signatures are in agreement with the CV results, where

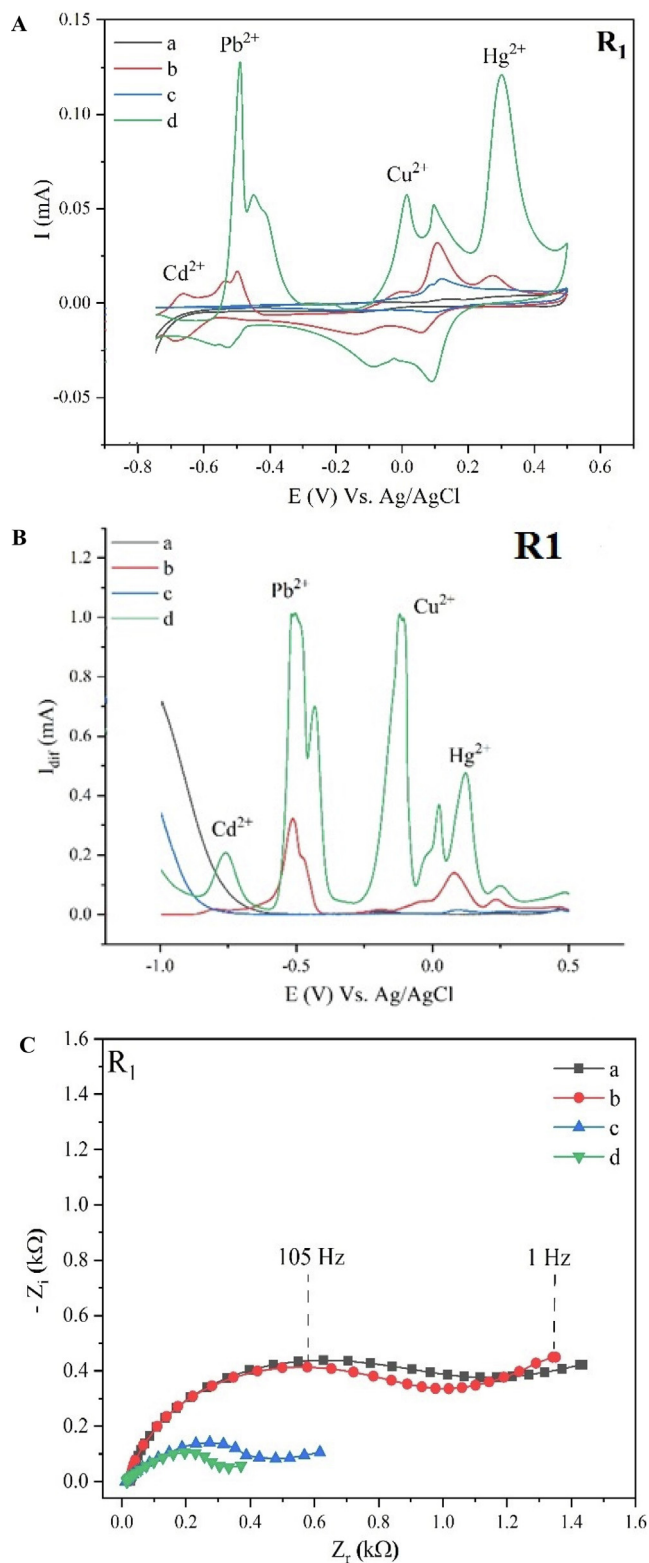


Fig. 5 Electrochemical characterization of (a) bare electrode in 0.2 M HCl, (b) bare electrode in the presence of 1 ppm each of heavy metals ions in 0.2 M HCl, (c) modified electrode in 0.2 M HCl, and (d) modified electrode in the presence of 1 ppm each of HMs in 0.2 M HCl through exploring the overlaid CV voltammograms (A), SWV signatures (B), and EIS Nyquist plots (C).

the bare (**a**) and modified electrode (**c**) did not represent any anodic signal. After adding the heavy metals to the medium, the appearance of net well-separated peaks of heavy metals ions centered at their pertaining potentials was noticed with enhanced current intensity when coming to the $R_1@SPE$ (**d**) compared to the bare gold electrode (**b**), meaning that the sensitivity of the electrode has increased notably after its modification, owing to the heavy metals accumulation on its surface, the high adsorption capacity and the large electroactive surface of resorcinarene platform.

EIS is one of the key measurement techniques to study the electrode–electrolyte interfaces.

The most common graphical representation of the EIS data is known as the Nyquist plot. A typical illustration of a Nyquist plot for an idealized faradaic reaction with a probe containing redox couple consists of a semicircle limited by the charge transfer elements (R_{ct}) and double-layer capacitor (CD) shifted on a real axis (Z_{real}) by the value of the solution resistance (R_s).

The value of R_{ct} relates to the radius of the semicircle. The resonance frequency of the parallel combination R_{ct} and CD matches with the highest imaginary impedance part of the curve (Z_{im}).

For higher frequencies, the diffusion effects do not play any significant role, while at low frequencies, the Warburg impedance cannot be neglected. Warburg impedance is related to the diffusion of ions to the oppositely charged electrode. In this case, HM ions in solution diffuse from the bulk fluid to the electrode and as a consequence, increase the Warburg impedance at low frequencies. This hinders the mobility of the slow alternating ions responding to an applied voltage. However, in a high-frequency region, ions have no time to diffuse to a distance before the reversal of an input voltage and thus Warburg impedance does not influence the system response (Dominguez-Benetton et al., 2012).

As mentioned above, Warburg impedance is the dominant parameter for the diffusion-controlled region as the redox couple lowers the charge transfer resistance R_{ct} . The further decrease of the frequency results in a transition from a semicircle to a straight 45° declined line at low frequencies. Adsorption of HMs composite from the analyte of interest to an electrode surface results in the building up of complexes, which are replicated by the changes in material property, i.e., dielectric constant and dependent electrical double-layer capacitor (Dominguez-Benetton et al., 2012).

However, the formation of complexes adsorbing at the electrode/electrolyte interface in the presence of redox couple can be measured by an increase in the R_{ct} value, since the thickness of an insulating layer including the composite and analyte increases or changes its density and thus disturbs a current flow into the electrodes. This is displayed as an extension of the semicircle to a nearly straight line as shown in (Fig. 5C).

As displayed in Fig. 5C, the Nyquist plots displayed a semicircle in the high frequencies associated with an electron transfer limited process, and a further line at low frequencies, indicating a diffusion-controlled process. In the case of bare electrodes (**a**) and (**b**), the semicircle diameter equal to the charge transfer resistance (R_{ct}) decreased after the addition of 1 ppm of HMs in 0.2 M HCl. Further decrease in R_{ct} was revealed after modifying the electrodes with R_1 (**c**) and (**d**). The smallest R_{ct} values were associated with the modified electrodes in the presence of 1 ppm of heavy metals ions in 0.2 M

HCl (**d**). The decrease in R_{ct} values of the modified electrode indicates the electrode surface conductivity improvement from one side and the enhanced electron transfer properties from another. In the present case, we demonstrated in (Fig. 5C) that the charge transfers rate increases even at OCP as a result of the chemical surface modification.

In future contributions, we plan to perform tests where impedance measurements are performed at fixed bias potentials, preferably at potentials corresponding to the maximum current peak of the tested ions. Since a significantly larger R_{ct} difference can be achieved at those potentials due to the influence of the investigated ions. Those measurements will be the basis for the development of alternative sensing methods based on the EIS measurements.

3.2.2. Optimization of the experimental parameters

The optimization of the experimental parameters was achieved to accomplish the best electroanalytical response, and therefore, the best analytical sensitivity. The parameters affecting heavy metals ions sensing were optimized by using SWV.

The supporting electrolyte, pH, accumulation potential, and accumulation time were adjusted to conclude the best conditions for achieving an enhanced detection (Fig. 6).

3.3. Effect of supporting electrolyte

The electrochemical detection of HM by the $R_1@SPE$ platform is pH-dependent. The selection of the proper supporting electrolyte and buffer is a significant step in electroanalytical tests because the electrolyte composition and pH influence the properties of the solution as well as the electrode/solution interface, modifying the kinetics and thermodynamics of the charge transfer process, and the adsorption at the electrode surface. Therefore, the pH influence on the electrochemical detection of HM using SWV as a detection technique was investigated.

The electrolytic solution plays a vital role in boosting the medium's conductivity where the electrochemical detection is taking place, supporting electrolytes viz. 0.2 M HCl ($pH_i = 0.7$), KCl 0.2 M ($pH_i = 6.8$), and ACB 0.2 M ($pH_i = 5.3$) were employed herein for selecting the appropriate one to be utilized in further detection investigations. In Fig. 6a, it was observed that the uppermost SWV current intensities were obtained utilizing 0.2 M HCl as an electrolytic medium, which is explained by its greater conductivity ensuring a fast charge transport process of the HMs and stabilizing them at the modified electrode's surface. Therefore, 0.2 M HCl was selected as the optimal supporting electrolyte to be used in further detection studies.

3.4. Effect of accumulation time

The effect of accumulation time on the square wave voltammetry signals was studied from 30 to 180 s (Fig. 6b), the current values increased upon the increase of accumulation time up to 90 s, owing to the progressive buildup of HMs on the modified electrode's surface. After 90 s, the current values dropped gradually due to the surface saturation process, meaning that the equilibrium conditions between the complexed heavy metals and those present in the electrolytic solution were achieved.

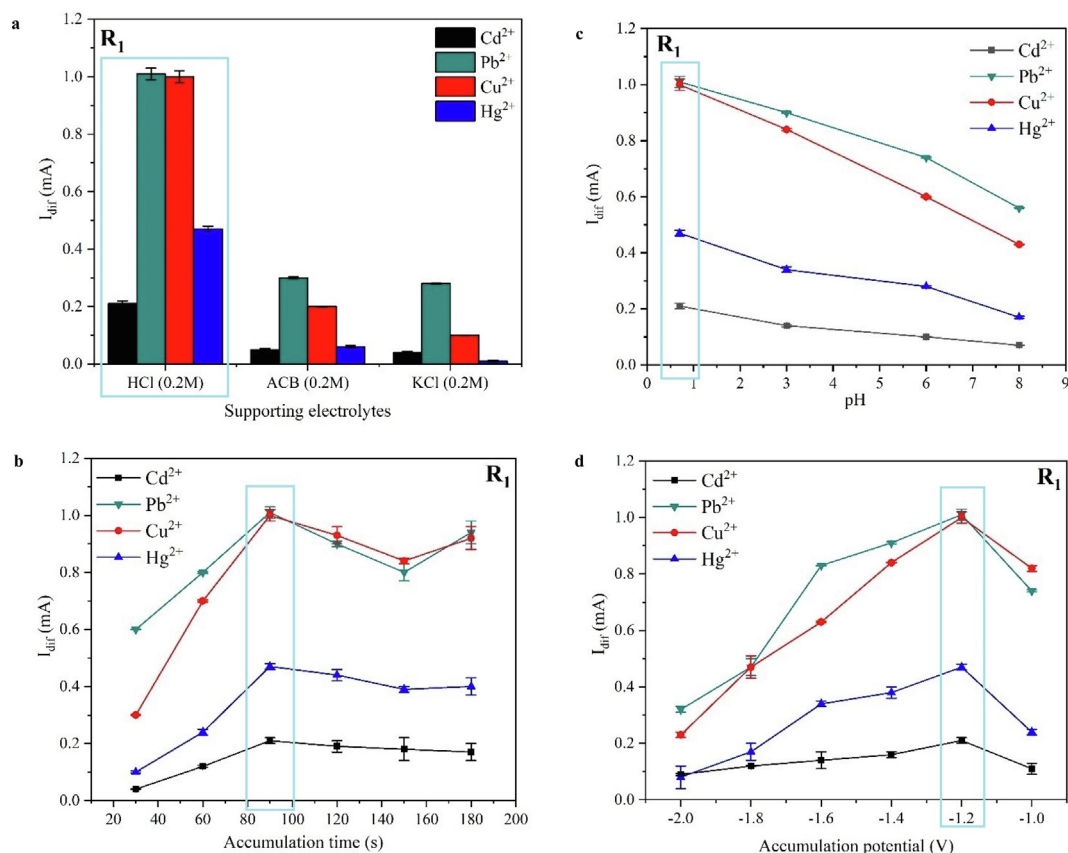


Fig. 6 Influence of various supporting electrolytes (a), accumulation time (b), pH (c), and accumulation potential (d) on the electrochemical SWV signals of the modified electrodes in presence of 1 ppm each of HMs.

The 90 s accumulation time was selected as optimal and was employed in further electrochemical examinations.

3.5. Effect of pH

The complexation process of the HMs within the $R_1@SPE$ platform is highly affected by the medium's pH. Hence, the sensing of HMs in HCl 0.2 M ($pH_i = 0.7$) has been examined by adjusting the pH values over a range from 0.7 to 8. The optimal pH of 0.2 M HCl for obtaining the highest SWV currents is 0.7 (Fig. 6c), which is applied in further SWV detection studies. However, while increasing the pH towards alkaline values, a decrease in the peak current values was observed for all HMs, explained by their hydrolysis and the formation of insoluble metal hydroxides on the electrode surface at higher pH values, causing current fluctuations and decrease.

3.6. Effect of accumulation potential

The influence of the accumulation potential on the SWV in the electrochemical determination of HMs was deliberate. The applied potential range was $-1V$ to $-2V$, (Fig. 6d), the peak currents of various HMs reached their maximum at $-1.2 V$. Once the potential is shifted towards more negative values, a decrease in the peak currents of HMs is observed. Generally, such a trend is explained by the hydrogen evolution reaction, this later was proved by the presence of bubbles on the electrode's surface during the measurements. So, an accumulation

potential of $-1.2 V$ was employed in further studies as optimal.

3.6.1. Electrochemical determination of HMs

The analytical performance of the proposed electrochemical sensor was examined under the concluded optimal conditions (0.2 M HCl, $pH = 0.7$), accumulation potential of $-1.2 V$ for an accumulation time of 90 s. Fig. 7a,b present the overlaid square wave voltammograms for the simultaneous electrochemical determination of HMs in the concentration range from 1 to 100 ppb based on the $R_1@SPE$, whereas the corresponding calibration curve is displayed. The peak separation in the SWV signals is large to quantify each metal ion distinctly. On the voltammograms of $R_1@SPE$, some peaks appeared apart from those corresponding to the HMs, owing either to non-complexed analytes trapped on the modified SPE surface (electroactive impurities formerly present in the electrolytic solution) or due to the resorcinarene leaching.

Based on the constructed calibration curve (Fig. 7b), a perfect linear relationship between the concentrations of HMs and the responses in SWV peak currents was established (Table 4). The limits of detection (LODs) and limits of quantification (LOQs) were calculated from $LOD = 3.3\sigma/S$ and $LOQ = 10\sigma/S$, respectively. Where σ is the standard deviation of the blank (based on three measurements) and S is the linear range's slope (the sensor's sensitivity).

The recommended sensor presented wide linear responses and noble sensitivities, the attained LODs and LOQs are much

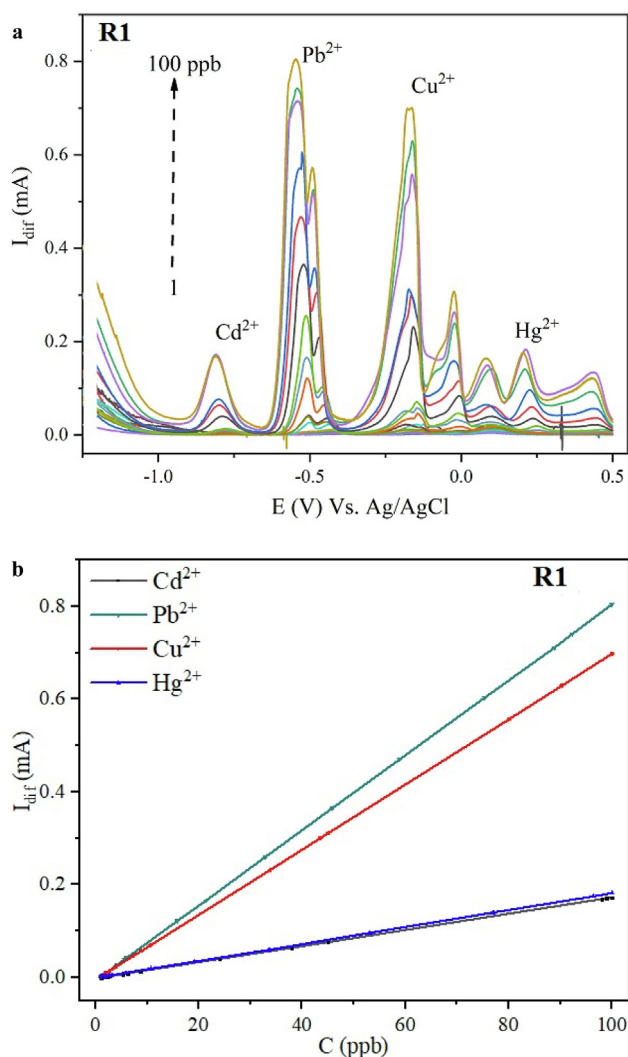


Fig. 7 (a) Simultaneous electrochemical determination of the studied HMs in the concentration range from 1 to 100 ppb under optimal conditions based on $R_1@SPE$ sensing platform, (b) the insert is presenting the corresponding calibration curve.

lower than the recommended thresholds stated by the WHO and the USEPA, therefore confirming the ultra-sensitivity of the sensing platform. The sensor has proven to be the most sensitive to lead and copper ions detection, nevertheless cadmium and mercury ions are also well measurable.

3.6.2. Interferences study

The effect of interfering ions on the HMs determination and the sensor's selectivity was investigated via adding metal ions

frequently present in water matrices, i.e. Al^{3+} , K^+ , Mg^{2+} , Zn^{2+} , and Ni^{2+} . A concentration of 4 ppm (40 folds) of each interfering ion was added to 0.2 M HCl ($pH = 0.7$) containing 100 ppb of heavy metals; Fig. 8 displays a comparison of the heavy metals peak currents for the developed sensor in the absence (control) and in the presence of interfering ions under the determined optimal conditions.

Based on the constructed calibration curves (Fig. 8), a linear relationship between the concentrations of heavy metals ions and the responses in peak currents was established (see correlation coefficients in Table 5). Evaluating Table 5, the calculated signal deviations of 100 ppb of heavy metals ions are less than 5%, so the studied interfering cations did not affect the simultaneous detection of HMs while applying the optimized procedure, which withstands the potential employment of the fabricated sensor for the simultaneous selective determination of heavy metals ions.

3.6.3. Consideration of reproducibility and repeatability

The repeatability, expressed as relative standard deviation (RSD %, $n = 3$) of the slope of the SWV calibration plot, was determined by measuring the analytical signal of HM ions over the concentration of 100 ppm using the $R_1@SPE$ modified platform, three successive scans.

Likewise, the sensor's reproducibility has been assessed employing 3 tests of $R_1@SPE$ modified electrodes to simultaneously detect 100 ppb of heavy metals ions.

The outcomes in terms of residual standard deviation (RSD) are tabulated in Table 6. The RSDs values are less than 5 %, which demonstrates excellent reproducibility and repeatability of the developed sensor platform, permitting its possible real application to determine trace levels of heavy metals ions simultaneously with high analytical selectivity.

3.6.4. Assessment of detection and quantification limits of the $R_1@SPE$ platform

The sensitivity and quantification limits of Cd^{2+} , Pb^{2+} , Cu^{2+} , and Hg^{2+} ions disclose significantly good sensitivity of the $R_1@SPE$ modified sensor as tabulated in Tables 3 and 6. The calculated sensitivity limits of the selected metal ions displayed a lower value than the sensitivity limits of numerous sensing platforms of modified electrodes described in the literature (Munir et al., 2019; Xiang et al., 2020; Mei C. J. and Ahmad S. A. A., 2021). As shown in Table 7, the sensitivity values of LOD, LOQ, RSD (Repeatability), and LR, of our $R_1@SPE$ based sensor, were favorable while the RSD (Reproducibility) values were slightly higher. Furthermore, our $R_1@SPE$ based sensor showed good stability, which is due to the insolubility of the modifying material in the water medium for the detection of metal ions. This enhanced stability is further designated by improved reproducibility.

Table 4 Metrological parameters of the developed electrochemical sensor.

| Ions | LR (ppb) | Fitting equation | R^2 | LOD (ppb) | LOQ (ppb) |
|-----------|----------|-------------------------------------|--------|-----------|-----------|
| Cd^{2+} | 1–100 | $I = 0.0017 * C_{Cd^{2+}} - 0.0016$ | 0.9999 | 0.37 | 1.11 |
| Pb^{2+} | 1–100 | $I = 0.0081 * C_{Pb^{2+}} - 0.0064$ | 0.9999 | 0.19 | 0.57 |
| Cu^{2+} | 1–100 | $I = 0.0070 * C_{Cu^{2+}} - 0.0049$ | 0.9999 | 0.23 | 0.70 |
| Hg^{2+} | 1–100 | $I = 0.0018 * C_{Hg^{2+}} - 0.0006$ | 0.9999 | 0.41 | 1.23 |

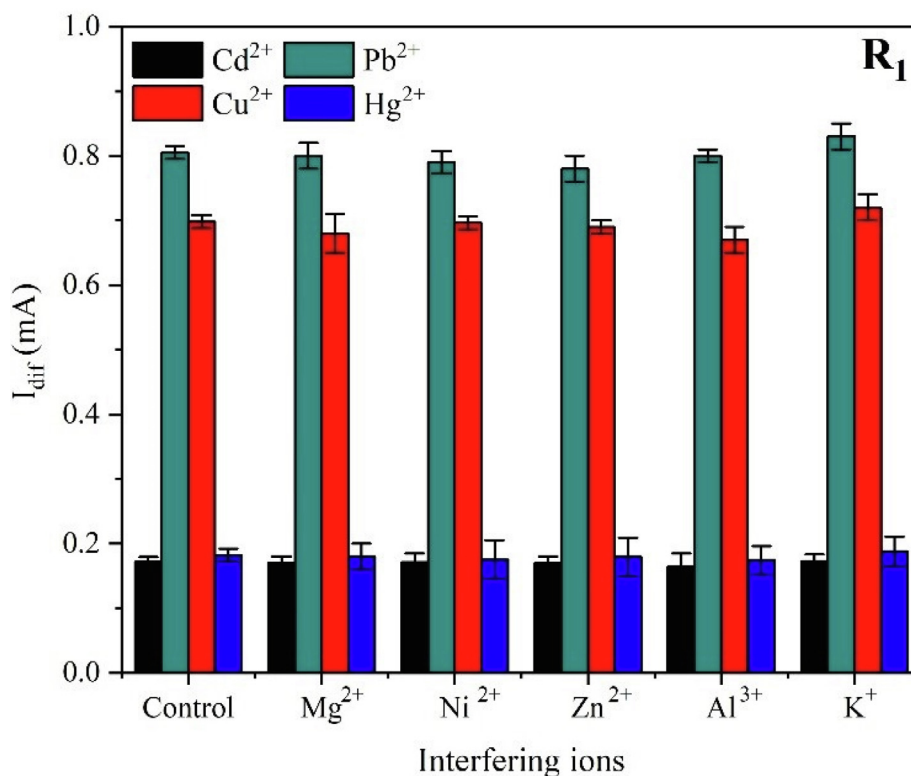


Fig. 8 Bar charts representing the heavy metals peak currents for the $R_1@SPE$ sensor in the absence (control) and the existence of interfering ions under optimal conditions.

Table 5 Current peak deviations for 100 ppb of heavy metals in the presence of 40 folds' excess of interfering ions.

| Interfering ions | Peak deviation (%) = $\left(\frac{I_{\text{control}} - I_{\text{control+interfering}}}{I_{\text{control}}}\right) \times 100$ | | | |
|------------------|---|-----------|-----------|-----------|
| | Cd^{2+} | Pb^{2+} | Cu^{2+} | Hg^{2+} |
| Mg^{2+} | 1.17 | 0.62 | 2.57 | 1.10 |
| Ni^{2+} | 0.58 | 1.86 | 0.30 | 3.84 |
| Zn^{2+} | 1.17 | 3.10 | 1.15 | 1.64 |
| Al^{3+} | 4.06 | 0.62 | 4.01 | - 4.40 |
| K^+ | - 0.60 | - 3.11 | - 3.15 | - 3.29 |

Table 6 Residual Standard Deviation (RSD) values related to reproducibility and repeatability of the developed electrochemical sensor.

| % RSD values related to: | Heavy metal ions | | | |
|---------------------------|------------------|-----------|-----------|-----------|
| | Cd^{2+} | Pb^{2+} | Cu^{2+} | Hg^{2+} |
| Reproducibility (3 tests) | 4.68 | 3.93 | 3.64 | 3.24 |
| Repeatability (3 tests) | 2.19 | 2.56 | 1.44 | 2.18 |

3.7. Heavy metals ions detection mechanisms

3.7.1. Piezogravimetric detection process

Numerous factors are involved in explaining the piezogravimetric detection mechanism, for instance, the complementarity

between the metal ions and the resorcinarene cavity size, besides the molecular structure of ligand (substituents nature and number). Potential complexation interactions between the sensing platform and target ions are mainly of a non-covalent physical nature (*VDW*, cation- π ...etc.). Herein, we enlighten the sensing mechanism in two major phases:

Table 7 Comparison of some figures of merits of the $\mathbf{R}_1@SPE$ platform with the reported the Cl-DPTU modified GCE modified electrodes (Munir et al., 2019) for sensing ability of Cd^{2+} , Pb^{2+} , Cu^{2+} , and Hg^{2+} ions.

| HM Ions | LOD (ppb) | LOQ (ppb) | % RSD (Reproducibility) | % RSD (Repeatability) | LR (ppb) |
|---|-----------|-----------|-------------------------|-----------------------|-----------|
| $\mathbf{R}_1@SPE$ sensor platform | | | | | |
| Cd^{2+} | 0.37 | 1.11 | 4.68 | 2.19 | 1–100 |
| Pb^{2+} | 0.19 | 0.57 | 3.93 | 2.56 | 1–100 |
| Cu^{2+} | 0.23 | 0.70 | 3.64 | 1.44 | 1–100 |
| Hg^{2+} | 0.41 | 1.23 | 3.24 | 2.18 | 1–100 |
| Cl-DPTU modified GCE modified electrodes (Munir et al., 2019). | | | | | |
| Cd^{2+} | 6.45 | 21.5 | 1.68 | 3.77 | 1–5000 |
| Pb^{2+} | 11.0 | 36.8 | 2.31 | 3.40 | 1–5000 |
| Cu^{2+} | 7.85 | 26.2 | 3.78 | 3.40 | 1.1–10000 |
| Hg^{2+} | 9.15 | 30.4 | 2.05 | 4.36 | 1–5000 |

The first phase manifesting in a complexation, or else host–guest interaction between the metals ions ($\text{M}^{n+} = \text{Cd}^{2+}$, Cu^{2+} , Hg^{2+} , and Pb^{2+}) and the resorcinarene (\mathbf{R}_1) already attached to the gold surface, either owing to an electron transfer from heteroatoms and nucleophilic elements towards HMs or due to their physical adsorption within the ligands' cavities, commonly these interactions are of *VDW* and cation- π origins:



The second stage is the simultaneous mass loading (accumulation) of metals ions on the solution-electrode interface and the piezogravimetric detection of the metal ions buildup on the resonator's surface.

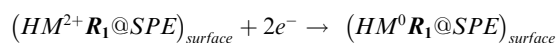
3.8. Electrochemical detection mechanism

The proposed sensing platform achieved low detection limits due to the analytical performance improvement; explained by the high complexation affinity between the heavy metals ions and the hydroxyl groups of the resorcinarenes, affording better conditions for a host–guest reaction, the suggested electrochemical mechanism can be clarified in three steps:

Accumulation: This step consists to accumulate the target metallic cations ($^{2+}$) on the electrode surface by adsorption, hence, it is a primordial condition that ensures good sensitivity and a higher detection afterward, the physical adsorption of charged heavy metals ions on the modified electrode's surface (SPE), is mainly performed via electrostatic attractions:

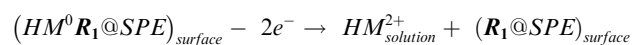


Pre-concentration: At a higher negative potential compared to that of the HM^{2+}/HM couples, the adsorbed heavy metals ions are electrodeposited on the modified SPE through a cathodic reduction from a valence state of ($^{2+}$) to (0) to enhance the mass transfer rate, permitting the HMs to be deposited at the SPE surface:



Stripping: The ions already electrodeposited on the electrode's surface are oxidized to ensure their dissolution back to the electrolyte, thus, yielding an analytic signal. Contrary to the preconcentration step, a positive scan has taken place to kinetically promote the separation and the consistent detection of the metallic ions, which led to well-defined voltam-

grams peaks with higher current intensities, in other words, the electrodeposited HMs are turned back to the electrolytic solution through anodic oxidation, translated by an SWV analytic signal. In this step, a positive scan took place for the consistent determination of the four heavy metals ions:



4. Conclusions

The ionophore (C-dec-9-enylcalix[4]resorcinarene) was synthesized and characterized and utilized as the recognition element for the $\mathbf{R}_1@SPE$ platform applying electrochemical (CV and SWV), and piezogravimetric (QCM-I) methods.

The developed $\mathbf{R}_1@SPE$ sensor displayed excellent sensing behavior towards heavy metals cations (Cd^{2+} , Hg^{2+} , Cu^{2+} , and Pb^{2+}) with good sensitivity, reproducibility, and repeatability, due to the strengths of the applied electrochemical and piezogravimetric methodologies which allowed the development of miniaturized platform sensors.

Decent metrological characteristics were gained from QCM-I frequency shifts outcomes, especially in the case of copper ions getting a LOD of 10 ppb, moreover, the sensor showed cadmium and mercury ionic selectivity. Additionally, the voltammetric $\mathbf{R}_1@SPE$ sensor could simultaneously detect the heavy metals ions under the optimized experimental conditions, and the lowest LOD was associated with Pb^{2+} (0.19 ppb).

The presence of common metal ions (Al^{3+} , K^+ , Mg^{2+} , Zn^{2+} , and Ni^{2+}) did not interfere with the simultaneous detection of Pb^{2+} , Cd^{2+} , Cu^{2+} , and Hg^{2+} within reasonable tolerance and offered suitable repeatability and reproducibility.

The obtained results in this work are strengthening the possibility of using QCM-I and voltammetric-based resorcinarene platforms in real-life detection and monitoring of heavy metals ions in water media.

Declaration of Competing Interest

The authors declare that they have no known competing financial interests or personal relationships that could have appeared to influence the work reported in this paper.

Acknowledgements

The support from the BIONANO_GINOP-2.3.2-15-216-00017 project, as well as the Stipendium Hungaricum Scholarship Program, is appreciated. Many thanks to MicroVacuum Ltd for loaning the QCM-I apparatus.

References

- Ahmadzadeh, S., Rezayi, M., Faghih-Mirzaei, E., Yoosefian, M., Kassim, A., 2015. Highly Selective Detection of Titanium (III) in Industrial Waste Water Samples Using Meso-octamethylcalix[4] pyrrole-Doped PVC Membrane Ion-Selective Electrode. *Electrochim. Acta* 178, 580–589. <https://doi.org/10.1016/j.electacta.2015.07.014>.
- Akl, M.A., Abd El-Aziz, M.H., 2016. Polyvinyl chloride-based 18-crown-6, dibenzo18-crown-6 and Calix-[6]-arene zinc(II)-potentiometric sensors. *Arab. J. Chem.* 9, S878–S888. <https://doi.org/10.1016/j.arabj.2011.09.009>.
- Aragay, G., Pons, J., Merkoçi, A., 2011. Recent Trends in Macro-, Micro-, and Nanomaterial-Based Tools and Strategies for Heavy-Metal Detection. *Chem. Rev.* 111, 3433–3458. <https://doi.org/10.1021/cr100383r>.
- Arfin T., 2021. 9-Emerging trends in lab-on-a-chip for biosensing applications, Editor(s): Chaudhery Mustansar Hussain, Sudheesh K. Shukla, Girish M. Joshi, In *Micro and Nano Technologies, Functionalized Nanomaterials Based Devices for Environmental Applications*, Elsevier, 199-218, <https://doi.org/10.1016/B978-0-12-822245-4.00008-8>.
- Arora, V., Chawla, H.M., Singh, S.P., 2007. Calixarenes as sensor materials for recognition and separation of metal ions. *Arkivoc* 2, 172–200.
- Aoyama, Y., Tanaka, Y., Sugahara, S., 1989. Molecular recognition. 5. Molecular recognition of sugars via hydrogen-bonding interaction with a synthetic polyhydroxy macrocycle. *J. Am. Chem. Soc.* 111, 5397–5404. <https://doi.org/10.1021/ja00196a052>.
- Bettazzi, F., Giorgi, C., Laschi, S., Palchetti, I., 2012. Dipyridine-Containing Macrocyclic Polyamine – Nafion-Modified Screen-Printed Carbon Electrode for Voltammetric Detection of Lead. *Electroanalysis* 24, 591–599. <https://doi.org/10.1002/elan.201100581>.
- Briand, E., Zach, M., Svedhem, S., Kasemo, B., Petronis, S., 2010. Combined QCM-D and EIS study of supported lipid bilayer formation and interaction with pore-forming peptides. *The Analyst* 135, 343. <https://doi.org/10.1039/B918288H>.
- Briffa, J., Sinagra, E., Blundell, R., 2020. Heavy metal pollution in the environment and their toxicological effects on humans. *Heliyon* 6, (9). <https://doi.org/10.1016/j.heliyon.2020.e04691> e04691.
- Cao, Z., Guo, J., Fan, X., Xu, J., Fan, Z., Du, B., 2011. Detection of heavy metal ions in aqueous solution by P(MBTVC-co-VIM)-coated QCM sensor. *Sens. Actuators B Chem.* 157, 34–41. <https://doi.org/10.1016/j.snb.2011.03.023>.
- Chaudhuri, A., Odelius, M., Jones, R.G., Lee, T.-L., Detlefs, B., Woodruff, D.P., 2009. The structure of the Au(111)/methylthiolate interface: New insights from near-edge x-ray absorption spectroscopy and x-ray standing waves. *J. Chem. Phys.* 130, <https://doi.org/10.1063/1.3102095> 124708.
- Chawla, H.M., Gupta, T., 2015. Novel bis-calix[4] arene-based molecular probe for ferric iron through colorimetric, ratiometric, and fluorescence enhancement response. *Tetrahedron Lett.* 56, 793–796. <https://doi.org/10.1016/j.tetlet.2014.12.078>.
- Chen, Q., Wu, X., Wang, D., Tang, W., Li, N., Liu, F., 2011. Oligonucleotide-functionalized gold nanoparticles-enhanced QCM-D sensor for mercury(II) ions with high sensitivity and tunable dynamic range. *Analyst* 136, 2572–2577. <https://doi.org/10.1039/C1AN00010A>.
- Deshmukh, M.A., Shirsat, M.D., Ramanaviciene, A., Ramanavicius, A., 2018. Composites Based on Conducting Polymers and Carbon Nanomaterials for Heavy Metal Ion Sensing. *Crit. Rev. Anal. Chem.* 48, 293–304.
- Dominguez-Benetton, X., Sevda, S., Vanbroekhoven, K., Pant, D., 2012. The accurate use of impedance analysis for the study of microbial electrochemical systems. *Chem. Soc. Rev.* 41, 7228–7246. <https://doi.org/10.1039/C2CS35026B>.
- Ebdelli, R., Rouis, A., Mlika, R., Bonnamour, I., Jaffrezic-Renault, N., Ben Ouada, H., Davenas, J., 2011. Electrochemical impedance detection of Hg²⁺, Ni²⁺ and Eu³⁺ ions by a new azo-calix[4]arene membrane. *J. Electroanal. Chem.* 661, 31–38. <https://doi.org/10.1016/j.jelechem.2011.07.007>.
- Echabaane, M., Rouis, A., Bonnamour, I., Ouada, H.B., 2013. Studies of aluminum (III) ion-selective optical sensor based on a chromogenic calix [4] arene derivative. *Spectrochim. Acta. A. Mol. Biomol. Spectrosc.* 115, 269–274.
- Eddaif, Larbi, Shaban, A., Szendro, I., 2019a. Calix[4]Resorcinarene Macrocycles Interactions with Cd²⁺, Hg²⁺, Pb²⁺, and Cu²⁺ Cations: a QCM-I and Langmuir Ultra-thin Monolayers Study. *Electroanalysis* elan.201900651. <https://doi.org/10.1002/elan.201900651>.
- Eddaif, L., Trif, L., Telegdi, J., Egyed, O., Shaban, A., 2019b. Calix[4]resorcinarene macrocycles: Synthesis, thermal behavior, and crystalline characterization. *J. Therm. Anal. Calorim.* <https://doi.org/10.1007/s10973-018-7978-0>.
- Eddaif, L., Shaban, A., Telegdi, J., Szendro, I., 2020. A Piezo-gravimetric Sensor Platform for Sensitive Detection of Lead (II) Ions in Water Based on Calix[4]resorcinarene Macrocycles: Synthesis, Characterization, and Detection. *Arab. J. Chem.* 13, 4448–4461. <https://doi.org/10.1016/j.arabj.2019.09.002>.
- Elkhatat, A.M., Soliman, M., Ismail, R., Ahmed, S., Abounahia, N., Mubashir, S., Fouladi, S., Khraishah, M., 2021. Recent trends of copper detection in water samples. *Bull Natl Res Cent* 45, 218. <https://doi.org/10.1186/s42269-021-00677-w>.
- Emir Diltemiz, S., Keçili, R., Ersöz, A., Say, R., 2017. Molecular Imprinting Technology in Quartz Crystal Microbalance (QCM) Sensors. *Sensors (Basel, Switzerland)* 17 (3), 454. <https://doi.org/10.3390/s17030454>.
- Erdemir, S., Tabakci, B., Tabakci, M., 2016. A highly selective fluorescent sensor based on calix[4]arene appended benzothiazole units for Cu²⁺, S²⁻ and HSO⁴⁻ ions in an aqueous solution. *Sens. Actuators B Chem.* 228, 109–116. <https://doi.org/10.1016/j.snb.2016.01.017>.
- Fadillah, G., Saputra, O.A., Saleh, T.A., 2020. Trends in Polymers Functionalized Nanostructures for Analysis of Environmental Pollutants. *Trends Environ. Anal. Chem.* e00084. <https://doi.org/10.1016/j.teac.2020.e00084>.
- Göde, C., Yola, M.L., Yılmaz, A., Atar, N., Wang, S., 2017. A novel electrochemical sensor based on calixarene functionalized reduced graphene oxide: Application to the simultaneous determination of Fe(III), Cd(II), and Pb(II) ions. *J. Colloid Interface Sci.* 508, 525–531. <https://doi.org/10.1016/j.jcis.2017.08.086>.
- Hajiaghbabaei, L., Tajmiri, T., Badii, A., Ganjali, M.R., Khaniani, Y., Mohammadi Ziarani, G., 2013. Heavy metals determination in water and food samples after preconcentration by a new nanoporous adsorbent. *Food Chem.* 141 (3), 1916–1922.
- Jin Mei, C., Ainliah Alang Ahmad, S., 2021. A review on the determination heavy metals ions using calixarene-based electrochemical sensors. *Arab. J. Chem.* 14, <https://doi.org/10.1016/j.arabj.2021.103303> 103303.
- Kenawy, I.M.M., Hafez, M.A.H., Akl, M.A., Lashein, R.R., 2000. Determination by AAS of some trace heavy metal ions in some natural and biological samples after their preconcentration using newly chemically modified chloromethylated polystyrene-PAN ion-exchanger. *Anal. Sci.* 16, 493–500.
- Laghrib F., Saqrane S., Lahrach S., El Mhammedi M. A. 2021. Best of advanced remediation process: treatment of heavy metals in water using phosphate materials, *International Journal of Environmental Analytical Chemistry*, 101:9, 1192–1208, DOI: 10.1080/03067319.2019.1678603.
- Li, M., Gou, H., Al-Ogaidi, I., Wu, N., 2013. Nanostructured sensors for detection of heavy metals: a review. *ACS Sustainable Chem. Eng.* 2013, 1, 7, 713–723. <https://doi.org/10.1021/sc400019a>.
- Lim, S.-R., Schoenung, J.M., 2010. Human health and ecological toxicity potentials due to heavy metal content in waste electronic

- devices with flat panel displays. *J. Hazard. Mater.* 177, 251–259. <https://doi.org/10.1016/j.jhazmat.2009.12.025>.
- Lotfi, B., Tarlani, A., Akbari-Moghaddam, P., Mirza-Aghayan, M., Peyghan, A.A., Muzart, J., Zadmand, R., 2017. Multivalent calix[4] arene-based fluorescent sensor for detecting silver ions in aqueous media and physiological environment. *Biosens. Bioelectron.* 90, 290–297. <https://doi.org/10.1016/j.bios.2016.11.065>.
- Luo, H., Chen, L.-X., Ge, Q.-M., Liu, M., Tao, Z., Zhou, Y.-H., Cong, H., 2019. Applications of macrocyclic compounds for electrochemical sensors to improve selectivity and sensitivity. *J. Incl. Phenom. Macrocycl. Chem.* 95, 171–198. <https://doi.org/10.1007/s10847-019-00934-6>.
- Mahajan B., 2021. Drinking Water Quality Standards (WHO Guidelines), online version, <https://civiconcepts.com/blog/drinking-water-quality-standards>.
- Mei, C.J., Ahmad, S.A.A., 2021. A review on the determination heavy metals ions using calixarene-based electrochemical sensors. *Arabian J. Chem.* 14, (9). <https://doi.org/10.1016/j.arabjc.2021.103303>
- Mokhtari, B., Pourabdollah, K., Dalali, N., 2011. Analytical applications of calixarenes from 2005 up-to-date. *J. Incl. Phenom. Macrocycl. Chem.* 69, 1–55.
- Munir, A., Shah, A., Nisar, J., Ashiq, M.N., Akhter, M.S., Shah, A. H., 2019. Selective and simultaneous detection of Zn²⁺, Cd²⁺, Pb²⁺, Cu²⁺, Hg²⁺ and Sr²⁺ using surfactant modified electrochemical sensors. *Electrochim. Acta* 323, <https://doi.org/10.1016/j.electacta.2019.134592> 134592.
- Naik, S.S., Lee, S.J., Theerthagiri, J., Yu, Y., Choi, M.Y., 2021. Rapid and highly selective electrochemical sensor based on ZnS/Au-decorated f-multi-walled carbon nanotube nanocomposites produced via pulsed laser technique for detection of toxic nitro compounds. *J. Hazard. Mater.* 418, <https://doi.org/10.1016/j.jhazmat.2021.126269> 126269.
- Nur Abdul Aziz, S.F., Zawawi, R., Alang Ahmad, S.A., 2018. An Electrochemical Sensing Platform for the Detection of Lead Ions Based on Dicarboxyl-Calix[4]arene. *Electroanalysis* 30, 533–542. <https://doi.org/10.1002/elan.201700736>.
- Pratiwi, R., Nguyen, M., Ibrahim, S., Yoshioka, N., Henry, C., Tjahjono, D., 2017. A selective distance-based paper analytical device for copper(II) determination using a porphyrin derivative. *Talanta* 174, 493–499. <https://doi.org/10.1016/j.talanta.2017.06.041>.
- Prochowicz, D., Kornowicz, A., Lewiński, J., 2017. Interactions of Native Cyclodextrins with Metal Ions and Inorganic Nanoparticles: Fertile Landscape for Chemistry and Materials Science. *Chem. Rev.* 117, 13461–13501. <https://doi.org/10.1021/acs.chemrev.7b00231>.
- Pujol, L., Evrard, D., Groenen-Serrano, K., Freyssinier, M., Ruffien-Cizsak, A., Gros, P., 2014. *Front Chem.* 30;2:19, 2014. <https://doi.org/10.3389/fchem.2014.00019>. eCollection.PMID: 24818124.
- Reimers, J.R., Ford, M.J., Halder, A., Ulstrup, J., Hush, N.S., 2016. Gold surfaces and nanoparticles are protected by Au(0)–thiol species and are destroyed when Au(I)–thiolates form. *Proc. Natl. Acad. Sci.* 113, E1424–E1433. <https://doi.org/10.1073/pnas.1600472113>.
- Reimers, J.R., Ford, M.J., Marcuccio, S.M., Ulstrup, J., Hush, N.S., 2017. Competition of van der Waals and chemical forces on gold–sulfur surfaces and nanoparticles. *Nat. Rev. Chem.* 1, 0017. <https://doi.org/10.1038/s41570-017-0017>.
- Sartore, L., Barbaglio, M., Borgese, L., Bontempi, E., 2011. Polymer-grafted QCM chemical sensor and application to heavy metal ions real-time detection. *Sens. Actuators B Chem.* 155, 538–544. <https://doi.org/10.1016/j.snb.2011.01.003>.
- Sauerbrey, G., 1959. Verwendung von Schwingquarzen zur Wugung dünner Schichten und zur Mikrowugung. *Z. Phys.* 155, 206–222. <https://doi.org/10.1007/BF01337937>.
- Shaban, A., Eddaif, L., 2020. Comparative study of a sensing platform via functionalized Calix[4]resorcinarene ionophores on QCM resonator as sensing materials for detection of heavy metal ions in aqueous environments. *Electroanalysis* elan.202060331. <https://doi.org/10.1002/elan.202060331>.
- Stewart, M., Phillips, N.R., Olsen, G., Hickey, C.W., Tipa, G., 2011. Organochlorines and heavy metals in wild-caught food as a potential human health risk to the indigenous Māori population of South Canterbury. *New Zealand. Sci. Total Environ.* 409, 2029–2039. <https://doi.org/10.1016/j.scitotenv.2011.02.028>.
- Taghvai-Ganjali S., Zadmand R., Zeyaei M., Rahnama K., Faridbod F., Ganjali M-R., 2009. Synthesis of a New Calix[4]Arene and Its Application in Construction of a Highly Selective Silver Ion-Selective Membrane Electrode, *Organic Chemistry International*, vol. 2009, Article ID 601089. <https://doi.org/10.1155/2009/601089>.
- Tang, Q., Jiang, D., 2015. Insights into the PhC≡C/Au Interface. *J. Phys. Chem. C* 119, 10804–10810. <https://doi.org/10.1021/jp508883v>.
- Theerthagiri, J., Lee, S.J., Karuppasamy, K., Arulmani, S., Veeralakshmi, S., Ashokkumar, M., Choi, M.Y., 2021. Application of advanced materials in sonophotocatalytic processes for the remediation of environmental pollutants. *J. Hazard. Mater.* 412, <https://doi.org/10.1016/j.jhazmat.2021.125245> 125245.
- US Environmental Protection Agency. 2022. <https://www.epa.gov/ground-water-and-drinking-water/table-regulated-drinking-water-contaminants>, (Accessed 1 Feb. 2022).
- Woo, S.H., Lee, D.S., Lim, S.-R., 2016. Potential resource and toxicity impacts from metals in waste electronic devices. *Integr Environ Assess Manag* 12, 364–370. <https://doi.org/10.1002/ieam.1710>.
- Wu, Y., Pang, H., Liu, Y., Wang, X., Yu, S., Fu, D., Chen, J., Wang, X., 2019. Environmental remediation of heavy metal ions by novel-nanomaterials: A review. *Environ. Pollut.* 246, 608–620. <https://doi.org/10.1016/j.envpol.2018.12.076>.
- Xiang H., Cai Q., Li Y., Zhang Z., Cao L., Li K., Yang H., 2020. Sensors Applied for the Detection of Pesticides and Heavy Metals in Freshwaters, *J. Sens.* 2020, article ID:8503491, 22. <https://doi.org/10.1155/2020/8503491>.
- Yang, J.-L., Yang, Y.-H., Xun, Y.-P., Wei, K.-K., Gu, J., Chen, M., Yang, L.-J., 2019. Novel Amino-pillar[5]arene as a Fluorescent Probe for Highly Selective Detection of Au³⁺ Ions. *ACS Omega* 4, 17903–17909. <https://doi.org/10.1021/acsomega.9b02951>.
- Yu, Y., Theerthagiri, J., Lee, S.J., Muthusamy, G., Ashokkumar, M., Choi, M.Y., 2021. Integrated technique of pulsed laser irradiation and sonochemical processes for the production of highly surface-active NiPd spheres. *Chem. Eng. J.* 411, <https://doi.org/10.1016/j.cej.2021.128486> 128486.
- Zaba, T., Noworolska, A., Bowers, C.M., Breiten, B., Whitesides, G. M., Cyganik, P., 2014. Formation of Highly Ordered Self-Assembled Monolayers of Alkynes on Au(111) Substrate. *J. Am. Chem. Soc.* 136, 11918–11921. <https://doi.org/10.1021/ja506647p>.